Journal of Power Sources 198 (2012) 117–121

Contents lists available at SciVerse ScienceDirect

Journal of Power Sources

journal homepage: www.elsevier.com/locate/jpowsour

Short communication

Intermediate-temperature fuel cells with amorphous $Sn_{0.9}In_{0.1}P_2O_7$ thin film electrolytes

Pilwon Heo, Tae Young Kim, Jinsu Ha, Kyoung Hwan Choi, Hyuk Chang, Sangkyun Kang*

Energy Lab, Samsung Advanced Institute of Technology, Samsung Electronics Co. Ltd., Mt 14-1, Nongseo-Dong, Giheung-Gu, Yongin-Si, Gyeonggi-Do 446-712, South Korea

ARTICLE INFO

Article history:
Received 16 August 2011
Received in revised form
27 September 2011
Accepted 28 September 2011
Available online 4 October 2011

Keywords:
Thin film
Proton conductor
Amorphous tin pyrophosphate
Intermediate-temperature fuel cell

ABSTRACT

The polymer electrolyte membrane fuel cells (PEMFCs) for vehicle and portable application are faced with challenges in reducing cost and the system volume. The need of low temperature operation and humidification are the root causes of the challenge. The development of electrolyte membranes capable to operate in intermediate temperatures of 200–400 °C without humidification is crucially required to overcome the challenges since such fuel cell provides a chance to reduce or remove Pt in electrode and no need of humidification results in simple system. In this paper, we report the first successful fabrication of fuel cell based on fully dense amorphous $Sn_{0.9}In_{0.1}P_2O_7$ (SIPO) proton conducting thin film electrolyte membrane formed by sputtering. The obtained thin film electrolyte exhibits extremely low area specific resistance (ASR) of 0.04 Ω cm^2 without any additional humidification at 200 °C. The densification degree of the thin film electrolyte was confirmed through the observation of microstructure and high open circuit voltages (OCVs) between 0.95 V and 1.05 V in the fuel cells based on the thin film electrolyte. The thin film fuel cell yielded a peak power density of 44 mW cm^{-2} with electrolyte thickness of 180 nm at 200 °C.

1. Introduction

The researches of fuel cell system for vehicle and portable applications have been mostly based on polymer electrolyte membrane fuel cell (PEMFC) due to its fast start up and the possibility of using alcohol fuel [1,2]. The most widely adopted electrolyte has been perfluorinated membrane such as Nafion® by DuPont, which consists of tetrafluoroethylene backbone having sulfonic group at the end. It is essential to keep the sulfonic group hydrated for the membrane to have proton conductivity. This requirement, however, is the root cause of PEMFC's major bottlenecks: the need of humidification and the use of expensive Pt catalyst. The first bottleneck keeps the operating temperature of PEMFC under 80 °C and the second bottleneck is an inevitable result from the low operating temperature.

Fuel cells running at higher temperatures without additional humidification will achieve low cost and high efficiencies at the same time. Such fuel cell operation will offer simpler water management compared to conventional PEMFCs including the elimination of the humidifier units from the fuel cell system [3]. Also, electrode reaction kinetics enhanced by the increased temperature allows the use of Pt-free electrodes [4,5] as well as the reduction of Pt loading [6,7]. In terms of operating temperature, the reforming of alcohol fuels to hydrogen can be integrated with fuel cell stack if the stack runs within the alcohol reforming temperature range, which is 200–400 °C [8,9]. It allows the efficient use of high energy density fuels, which is particularly beneficial for transportation applications. It has been reported that the solid oxide fuel cells using proton conducting perovskite oxides, such as yttrium doped barium cerate [10,11] and yttrium doped barium zirconate [12,13] as an electrolyte are operable at 400 °C. Their performance, however, rapidly decrease under 400 °C. Thus, development of electrolyte membranes capable to operate in intermediate temperature (200–400 °C) without humidification is an essential element in overcoming the bottlenecks of current PEMFC technology.

The electrolyte materials for the intermediate-temperature fuel cells (ITFCs) have been extensively investigated. They usually consist of phosphate-based proton conductors such as CsH_2PO_4 [14], NH_4PO_3 [15] and SnP_2O_7 [16]. Recently, various metal pyrophosphates (MP_2O_7, where M = Sn [16–19], Ce [20], Zr [21]) have been reported to show good proton conductivity in the intermediate temperatures under unhumidified conditions. In particular, of these, $Sn_{0.9}In_{0.1}P_2O_7$ (SIPO) exhibited relatively high proton conductivities above 10^{-2} S cm^{-1} around 200 °C. However, the electrolyte membranes used for a fuel cell were prepared by pressing calcined $Sn_{0.9}In_{0.1}P_2O_7$ powders into pellets. Further reduction

* Corresponding author. Tel.: +82 31 280 9433; fax: +82 31 280 9359.
E-mail address: sangkyun.kang@samsung.com (S. Kang).

0378-7753/$ – see front matter © 2011 Elsevier B.V. All rights reserved.
doi:10.1016/j.jpowsour.2011.09.094

of the pressed pellet thickness was not achieved due to gas leakage through the pores of the pressed pellets. Also, it is hard to prepare fully sintered SIPO compacts due to the poor sinterability of phosphate based solid acid electrolytes. In order to enhance ionic conduction and cell performances, it was necessary to improve densification of the electrolyte through adopting more effective preparation methods. To synthesize thinner (<100 μm) but dense SIPO membrane, composite approach, in which the membranes are formed by mixing organic and inorganic materials, has been tried [22,23]. The increase of organic material contents improved tensile strength of the composite membrane, however, it reduced the conductivity of the composite membrane under unhumidified conditions. The operating temperature of ITFCs using the composite membrane is limited to below 200 °C due to the insufficient thermal stability of the organic materials. However, the fuel cell operation above 200 °C is desirable to fully utilize the advantages in ITFCs.

In this study, the fabrication and functionality of fully dense amorphous SIPO proton conducting thin film electrolyte membrane and the fuel cell based on the thin film membrane have been demonstrated for the first time. The area specific resistance (ASR) and fuel cell performances were evaluated using optimized thin film electrolyte with electrolyte thickness of 180–420 nm without humidification at 200 °C. The densification degree of the obtained thin film electrolyte was confirmed through the observation of microstructure and high open circuit voltages (OCVs) between 0.95 V and 1.05 V in the fuel cells.

2. Experimental

2.1. Preparation of materials and devices

Synthesis of SIPO powder: SIPO powder was prepared in similar manner as reported in the literature [16]. SnO_2 (99.99%, Aldrich) and In_2O_3 (99.99%, Aldrich) powders were mixed with 85% H_3PO_4 (Aldrich) and ion-exchanged water. The mixture solution was held with stirring at 300 °C until a high viscosity paste was formed. The pastes were calcined in an alumina pot at 650 °C in air for 2.5 h and then ground with a mortar and pestle to the form of powder.

Preparation of $Sn_{0.9}In_{0.1}P_2O_7$ target: The calcined SIPO powder was further ground in ethanol using a planetary mill with a zirconia mill container and zirconia balls for 14 h. The powder was mixed with 1 wt.% polyvinyl alcohol as a binder in a mortar and pressed at 1.5×10^3 kgf cm^{-2} to form a disk (2 in. diameter, 5 mm thick). After debinding at 500 °C for 12 h, the disk was sintered at 1200 °C for 2 h in air. The $Sn_{0.9}In_{0.1}P_2O_7$ target was completed by bonding the sintered disk with a copper backing plate using a conductive silver epoxy.

Fabrication of SIPO thin film: The thin film electrolyte was fabricated by RF sputtering with the SIPO target. The deposition was carried out with a power of 30–90 W in Ar and O_2/Ar mixture at a total pressure of 0.67–1.33 Pa. The substrate temperature was varied from room temperature to 700 °C during deposition and the target-to-substrate distance was changed in the range of 70–120 mm.

Fabrication of conductivity measurement cell and working fuel cell: For conductivity measurement cell, a dense Pt layer was deposited on a Si (1 0 0) wafer by RF sputtering with 50 W power in 0.67 Pa Ar atmosphere and followed by deposition of the SIPO thin film electrolyte and the dense Pt layer in the same condition as described above. The thicknesses of the Pt layers were 100 nm and electrolyte layer was 420 nm. The thin film fuel cells were formed with 200 nm thick porous Pt anode, 180–420 nm thick SIPO electrolyte, and 170 nm thick porous Pt cathode (area: 2.25 mm^2) on an anodic aluminum oxide (Synkera Technology Inc., 80 nm pores, 15% porosity) substrate. The sputtering of the porous Pt layer was carried out at 100 W power in 0.67 Pa Ar for anode and at 150 W power in 6.67 Pa Ar for cathode, respectively.

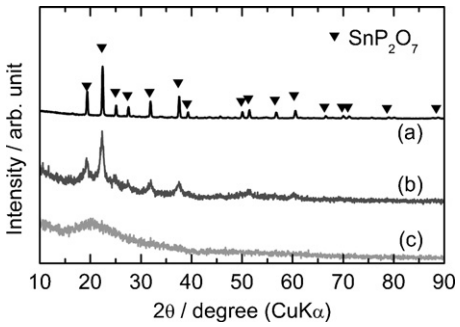

Fig. 1. XRD patterns of (a) $Sn_{0.9}In_{0.1}P_2O_7$ target, (b) SIPO thin film with post-heat treatment at 700 °C in air, and (c) SIPO thin film deposited on a heated substrate at 600 °C without post-heat treatment.

2.2. Measurement and characterization

Conductivity and ASRs of the SIPO thin film electrolytes were measured by using AC impedance spectroscopy in the frequency range of 0.1–10^6 Hz and the amplitude of 10 mV. The test was performed in unhumidified air ($P_{H_2O} = \sim 0.0075$ atm) with the measurement setup for the four probe method. For the fuel cell tests, the fabricated cells were attached on the custom made hydrogen feeding chamber and sealed by applying ceramic adhesive (Aremco Products, Inc., CP4010). The anode was electrically connected with Pt wire via silver paste. The cathode current collection was achieved by contacting a microprobe on the cathode. The whole test jig was placed inside of a temperature controlled oven. Dry pure H_2 and unhumidified air were supplied to the anode side and the cathode side with the flow rates of 50 and 100 SCCM, respectively. The crystalline structure was characterized by X-ray diffraction (XRD, Philips, XPert PRO). The morphology of cross-section of the films was observed by scanning electron microscopy (SEM, Hitachi, S5500) and transmission electron microscopy (TEM, FEI, Titan F30). The chemical composition of the thin film electrolytes was confirmed by X-ray photoelectron spectroscopy (XPS, Physical Electronics, Quantum 2000). Fourier transform infrared (FT-IR) spectra of the thin film electrolytes were measured in the transmission mode using Varian 670-IR Spectrometer.

3. Results and discussion

The results of SIPO thin film deposition revealed that the vacuum pressure and sputter power were the most crucial process parameters to control the densification of the SIPO films. Relatively dense films were achieved when the pressure was 0.67 Pa and the power was 60 W. For the control of crystallinity and chemical composition in the thin film, the substrate temperature was varied during the deposition and an additional heat-treatment of the deposited film was carried out as needed. From XRD patterns of SIPO target and deposited SIPO films (Fig. 1), it can be found that a crystalline SIPO film is fabricated by post-heat treatment of the deposited film at 700 °C and higher in air. The heat treated film as well as the sputter target showed consistent peaks representing the SnP_2O_7 cubic structure. The secondary crystal phase containing In dopant such as In_2O_3 was not detected. It suggests that doped In^{3+} was completely substituted for Sn^{4+}. However, as shown in Fig. 2a, the heat treated film was not dense enough with the existence of some defects. The defects generally lead to fuel crossover and sometimes cause short circuit when metal electrodes are formed on both sides of submicron ceramic electrolyte [13]. It is considered that the defects are formed by evaporation of phosphorus species during the post-heat

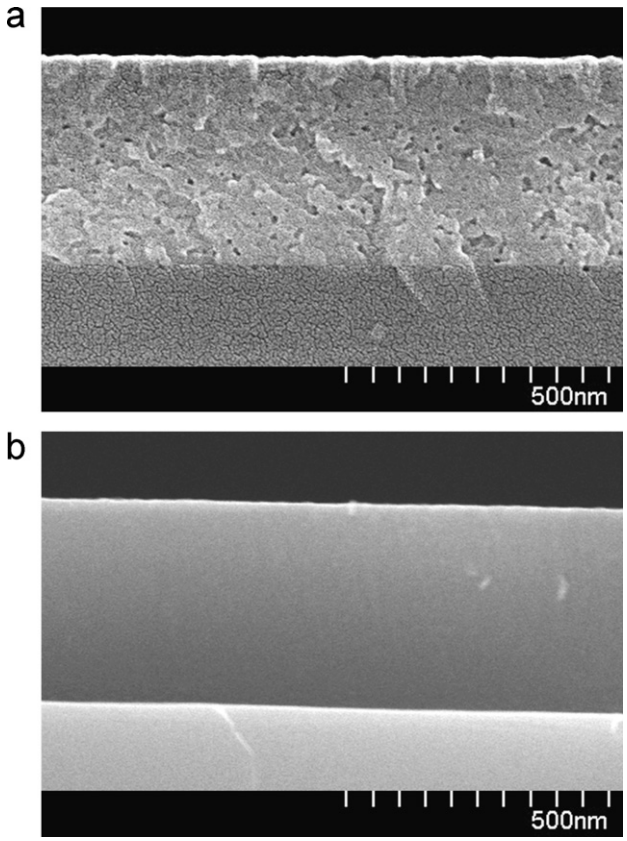

Fig. 2. SEM image of the cross-section of (a) crystalline and (b) amorphous SIPO films on a Si substrate. Crystalline SIPO film was fabricated by post-heat treatment at 700 °C in air. Amorphous SIPO film was deposited on a heated substrate at 600 °C without post-heat treatment.

treatment considering the decrease of phosphorus composition by the heat treatment. This may be one of reasons that the fully dense sintered compact of bulk phosphates have not been made. On the other hand, fully dense films were obtained by forming amorphous state of SIPO. The substrate was heated between room temperature and 700 °C during the deposition. The deposited thin film showed no diffraction peak state in the XRD result, regardless of substrate temperatures. Contrary to crystalline films, the amorphous thin films have no defects or pores (Fig. 2b).

The chemical composition of the films deposited with various sputter conditions was confirmed by XPS. As shown in Table 1, the composition ratio of Sn and In was consistent with that of the target (Sn:In = 0.9:0.1) regardless of sputtering conditions. However, composition ratio of phosphorus to metals, i.e. P/(Sn + In), varied with the sputter conditions. Among them, it was found that sputter atmosphere is an important factor to control the P/(Sn + In) ratio. The film deposited in Ar atmosphere, which denoted by Ar-film, indicated low phosphorus content; P/(Sn + In) = 1.6. The film deposited in 20% O_2 atmosphere, which denoted by O_2-film, was near the stoichiometry of $Sn_{0.9}In_{0.1}P_2O_7$; P/(Sn + In) = 2.0. This indicates that oxygen functions as reactant gas for the formation of P_2O_7 unit.

As shown in Fig. 3, the thin films exhibited similar conductivity behavior to that of bulk SIPO as reported in literatures [16,18], i.e. the conductivity increased with increasing temperature up to around 200 °C and slightly decreased with further increase of temperature. This implies that proton conduction mechanism in the amorphous SIPO thin film is similar to that in the bulk SIPO. It has been proposed that protons are incorporated in these metal pyrophosphates by interaction between water vapor and oxygen

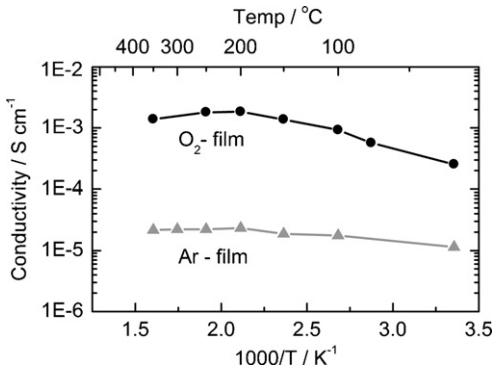

Fig. 3. Temperature dependence of conductivity of amorphous SIPO thin films (O_2-film and Ar-film). These conductivities were measured in unhumidified air (P_{H_2O} = ~0.0075 atm).

vacancies formed by the substitution of In^{3+} for Sn^{4+} in SnP_2O_7. And then the protons migrate via the dissociation of OH bonds in the P_2O_7 unit, which is called hopping mechanism [16]. The proton conduction in the amorphous thin films is supported by the observation of P–O···H group in Fourier transform infrared (FT-IR) analysis. The IR spectra of the thin films (Fig. 4) indicated the absorption peaks for P–O vibration (1150 cm^{-1} and 950 cm^{-1}) and P–O–P vibration (750 cm^{-1}) [24,25]. Also, P–O···H group was confirmed as the absorption band appeared at 3000–3600 cm^{-1}, which is the evidence of δ(OH) [26]. These results suggest that protons are bonded to Sn–P–O network formed in the amorphous thin films.

The conductivity of the Ar-film with lower phosphorus composition was much lower than the O_2-film with near stoichiometric phosphorus composition (P/(Sn + In) = 2); they were 2.32×10^{-5} S cm^{-1} and 1.85×10^{-3} S cm^{-1} at 200 °C for the Ar-film and the O_2-film, respectively. In addition, the absorption peaks for P–O and P–O–P vibrations were smaller in the Ar-film than in the O_2-film. Therefore, it is regarded that the P_2O_7 network for the proton conduction was formed in the amorphous thin films and the lower conductivity of the Ar-film is due to the phosphorus deficiency. During the sputtering, SIPO is transferred from the target to sample in a form of SIPO cluster rather than decomposed elements such as P, Sn and In. Thus, the Ar-film is expected to maintain phosphate structure even with phosphorus deficiency. Such phosphorus deficiency causes a partial disconnection of the P_2O_7 network for proton conduction, leading to the low conductivity [27].

The SIPO thin film implements low ASR and high OCV at the same time, which has not been the case of SIPO pellets and SIPO-based composites (Fig. 5). The amorphous SIPO thin film was deposited on a heated substrate at 600 °C without post-heat treatment. The results for the pellet and composite membrane were cited from the previous reports [22]. A decrease of the ASR for the pellet sample was achieved by reducing the electrolyte thickness but it resulted in

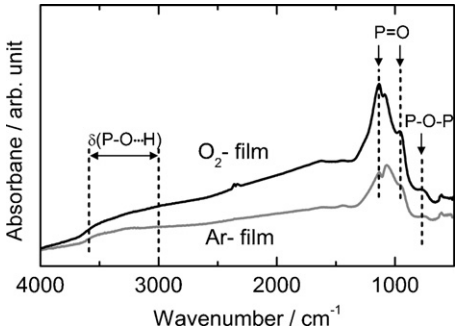

Fig. 4. FT-IR spectra of amorphous SIPO thin films.

Table 1
Chemical composition of SIPO films deposited with various sputter conditions. For all conditions, sputter power is 60 W and total pressure of sputter atmosphere is 5 mTorr.

Sputter condition			Composition		
Target–substrate distance	Substrate temperature	Sputter atmosphere	Sn	In	P
70 mm	Room temp.	10% O_2 in Ar	0.90	0.10	2.12
120 mm	Room temp.	10% O_2 in Ar	0.90	0.10	2.55
120 mm	600 °C	10% O_2 in Ar	0.90	0.10	2.18
120 mm	600 °C	0% O_2 in Ar	0.91	0.09	1.61
120 mm	600 °C	20% O_2 in Ar	0.90	0.10	2.03

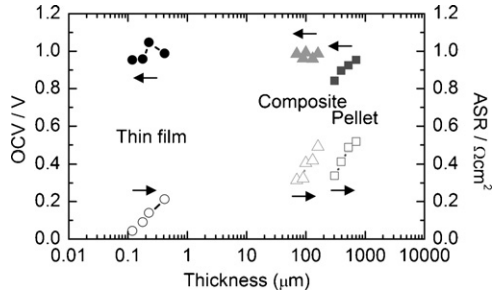

Fig. 5. Comparison of ASR (◯, □, △) and OCV (●, ■, ▲) at 200 °C for the thin film(◯, ●), pellet (□, ■), and composite membranes (△, ▲) consisting of SIPO. The results for the pellet and composite membranes were cited from the literature [22].

a decrease of the OCVs due to the fuel and air crossover through the electrolyte via defects such as pin-hole, crack, and pores. In contrast, the composite membrane consisting of the mixture of SIPO powder and polymer binders maintained high OCV (0.95 V) even when the thickness was reduced to 60 μm. Its lowest ASR was 0.24 Ω cm^2.

In the sputtered SIPO thin film, a significant decrease in the ASR has been achieved without a decrease in the OCV. The ASR for the thin film decreased to 0.04 Ω cm^2 by reducing electrolyte thickness to 180 nm. In spite of the fact that these films are ultra thin, fuel cells using the thin films yielded high OCVs of 0.95–1.05 V. This result is not only the direct evidence of the proton conduction in the present thin film, but also the film being dense and defect-free. The conductivity of the SIPO thin film is lower than those of the reported bulk pellet samples by one order of magnitude [16,19]. It is considered that the lower conductivity is due to the crystal structural irregularity in the amorphous materials. Crystalline SnP_2O_7 shows a cubic structure with SnO_6 octahedra and P_2O_7 units at the corners and the edges, respectively [16]. Such closely packed P_2O_7 units provide many proton bonding sites and associated transport pathways in the bulk. In amorphous SIPO, crystal structural regularity may not be as high as the regularity in bulk SIPO. In spite of lower conductivity, much lower ASR has been obtained in the amorphous SIPO thin film by making the SIPO electrolyte to a sufficiently thin and dense film. Furthermore, the SIPO thin film has the lowest ASR compared to the reported thin film proton conductors operating at the intermediate temperatures (of 200–400 °C), including 130 nm thick

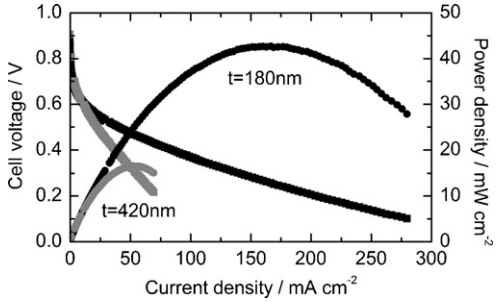

Fig. 6. Performance of a H_2/air fuel cell using SIPO thin film electrolyte with different thicknesses at 200 °C.

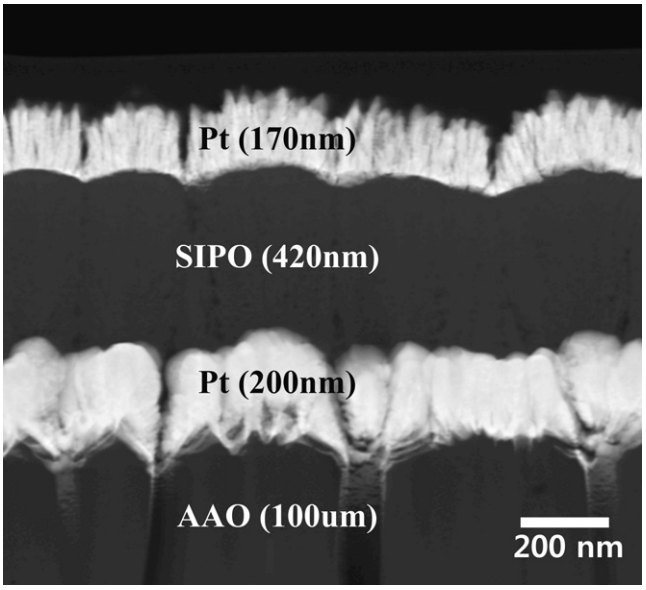

Fig. 7. TEM image of the cross-section of a SIPO thin film cell.

Y^{3+} doped zirconium phosphate (ASR = 0.085 Ω cm^2 at 340 °C) [28], 120 nm thick α-$Al_{0.1}Si_{0.9}O_x$, (ASR = 0.24 Ω cm^2 at 400 °C) [29], and 700 nm thick $BaCe_{0.8}Y_{0.2}O_{3-\delta}$ (ASR = 0.12 Ω cm^2 at 400 °C) [11].

For the fuel cell test, the following thin film fuel cell was fabricated by sputtering on a porous alumina substrate:

Ptanode(200 nm)|SIPOelectrolyte(180–420 nm)|Ptcathode(170 nm)

The current–voltage curves of the fuel cell with different electrolyte thickness are shown in Fig. 6. The peak power density of 16 mW cm^{-2} was achieved with 420 nm thick electrolyte and it was enhanced to 44 mW cm^{-2} by reducing the electrolyte thickness to 180 nm at 200 °C. However, the obtained power densities were low considering the ASR of the electrolyte. The voltage drop of the fuel cell with 420 nm thick electrolyte was 690 mV at a current density of 70 mA cm^{-2}. According to an EIS measurement of the cell, the ohmic resistance was 0.17 Ω cm^2. The corresponding voltage drop was only 12 mV. Thus, the low performance is attributed to large polarization resistance of electrodes. The present electrodes were solely composed of particles or aggregates of Pt in contact with the electrolyte only at its edge surface and the Pt electrodes show little porosity distribution as shown in TEM image of cell structure (Fig. 7), resulting in limited reaction sites and poor gas diffusion in the electrodes. Therefore, electrode structures with a higher porosity and an impregnation of the electrolyte to the electrodes will further improve the cell performance.

4. Conclusions

Amorphous SIPO proton conducting thin film electrolyte membranes and their fuel cells were fabricated by sputtering. The lowest

ASR of the amorphous SIPO thin film was 0.04 $\Omega\,cm^2$ at 200 °C without additional humidification. The defect-free microstructure in the thin film and the high OCV (>0.95 V) of the thin film fuel cell demonstrated the high densification degree of the thin film electrolyte. Also without humidification, the fuel cell with 180 nm thick amorphous SIPO electrolyte yielded a maximum power density of 44 $mW\,cm^{-2}$ at 200 °C. The performance of the SIPO thin film fuel cell will increase with the improvement of electrodes.

References

[1] B.C.H. Steele, A. Heinzel, Nature 414 (2001) 345.
[2] K. Lee, L. Zhang, J. Zhang, J. Power Sources 165 (2007) 108.
[3] Q. Li, R. He, J.O. Jensen, N.J. Bjerrum, Chem. Mater. 15 (2003) 4896.
[4] Y. Shao, G. Yin, Z. Wang, Y. Gaob, J. Power Sources 167 (2007) 235.
[5] P. Heo, K. Ito, A. Tomita, T. Hibino, Angew. Chem. Int. Ed. 47 (2008) 7841.
[6] R. Vellacheria, S.M. Unnia, S. Nahireb, U.K. Kharulb, S. Kurungot, J. Power Sources 195 (2010) 3425.
[7] T. Harada, Y.C. Jin, P. Heo, T. Hibino, Fuel Cells 10 (2010) 798.
[8] D.J.L. Bretta, A. Atkinson, D. Cumming, E. Ramirez-Cabrera, R. Rudkin, N.P. Brandon, Chem. Eng. Sci. 60 (2005) 5649.
[9] C. Pan, R. He, Q. Li, J.O. Jensen, N.J. Bjerrum, H.A. Hjulmand, A.B. Jensen, J. Power Sources 145 (2005) 392.
[10] S. Yamaguchi, T. Shishido, H. Yugami, S. Yamamoto, S. Hara, Solid State Ionics 162–163 (2003) 291.
[11] N. Ito, M. Iijima, K. Kimura, S. Iguchi, J. Power Sources 152 (2005) 200.
[12] J.H. Shim, J.S. Park, J. An, T.M. Gür, S. Kang, F.B. Prinz, Chem. Mater. 21 (2009) 3290.
[13] S. Kang, P. Heo, Y.H. Lee, J. Ha, I. Chang, S.W. Cha, Electrochem. Commun. 13 (2011) 374.
[14] D.A. Boysen, T. Uda, C.R.I. Chisholm, S.M. Haile, Science 303 (2004) 68.
[15] T. Matsui, S. Takeshita, Y. Iriyama, T. Abe, Z. Ogumi, J. Electrochem. Soc. 152 (2005) A167.
[16] Y.C. Jin, Y.B. Shen, T. Hibino, J. Mater. Chem. 20 (2010) 6214.
[17] M. Nagao, M. Takahashi, T. Hibino, Energy Environ. Sci. 3 (2010) 1934.
[18] X. Chen, C. Wang, E.A. Payzant, C. Xia, D. Chud, J. Electrochem. Soc. 155 (2008) B1264.
[19] X. Wu, A. Verma, K. Scott, Fuel Cells 8 (2008) 453.
[20] X. Sun, S. Wang, Z. Wang, X. Ye, T. Wen, F. Huang, Solid State Ionics 179 (2008) 1138.
[21] W.H.J. Hogarth, J.C.D. da Costa, J. Drennan, G.Q. Lu, J. Mater. Chem. 15 (2005) 754.
[22] P. Heo, M. Nagao, T. Kamiya, M. Sano, A. Tomita, T. Hibino, J. Electrochem. Soc. 154 (2007) B63.
[23] Y.C. Jin, K. Fujiwara, T. Hibino, Electrochem. Solid-State Lett. 13 (2010) B8.
[24] P.S. Attidekou, P.A. Connor, P. Wormald, D.P. Tunstall, S.M. Francis, J.T.S. Irvine, Solid State Ionics 175 (2004) 185.
[25] Y. Aoki, K. Ogawa, H. Habazaki, T. Kunitake, Y. Li, S. Nagata, S. Yamaguchi, Chem. Mater. 22 (2010) 5528.
[26] M. Nagao, T. Kamiya, P. Heo, A. Tomita, T. Hibino, M. Sano, J. Electrochem. Soc. 153 (2006) A1604.
[27] A. Tomita, N. Kajiyama, T. Kamiya, M. Nagao, T. Hibino, J. Electrochem. Soc. 154 (2007) B1265.
[28] Y. Li, T. Kunitake, Y. Aoki, E. Muto, Adv. Mater. 20 (2008) 2398.
[29] Y. Aoki, E. Muto, S. Onoue, A. Nakao, T. Kunitake, Chem. Commun. (2007) 2396.